CERN–PPE/95–129
28 August 1995

MEASUREMENTS OF THE STRONG COUPLING CONSTANT AND TESTS OF THE STRUCTURE OF QCD

Michael Schmelling, CERN

Abstract

Tests of perturbative QCD from many different reactions and over a large energy range are reviewed. The strong coupling constant is found to evolve with energy as predicted by QCD. The global average is consistent with the current PDG average $\alpha_s(M_Z) = 0.117 \pm 0.005$. The structure of QCD agrees with the expectation from a gauge theory based on an unbroken SU(3) symmetry underlying the interaction between spin 1/2 quarks and spin 1 gluons. Within an error of 2.5% the strong coupling is found to be flavour independent. The colour factor ratios are measured as $C_A/C_F = 2.221 \pm 0.225$ and $T_F/C_F = 0.353 \pm 0.132$, compatible with the SU(3) prediction.

Invited talk given at the
XV International Conference on Physics in Collision
Cracow, Poland, June 8–10, 1995.

1 Introduction

After the quark model was introduced by Gell-Mann and Zweig to explain the observed hadron multiplets in terms of fundamental constituents, deep-inelastic scattering experiments revealed a partonic structure of the nucleon. Further analysis established the QPM [1], showing that the partons carry the quantum numbers of the quarks, i.e. spin 1/2 and fractional electric charge. As more information was collected, however, problems ocured: The 4-momentum carried by the quarks inside the nucleon did not add up to the total 4-momentum of the nucleon, giving evidence for additional constituents which do not carry electric of weak charge. Unexpectedly large scaling violations in the structure functions of the nucleon were observed, showing that the partons inside are subject to a much stronger interaction than pure QED. Finally, assuming the quarks carry only the quantum numbers expected within the simple QPM implied the Pauli principle to be violated in bound states of three identical quarks like the Ω^-, the Δ^{++} or the Δ^-. To restore the Pauli principle, three internal degrees of freedom, labelled "colour", were required [2]. The same number was needed to understand the π^0 decay rate in the context of the QPM [3]. If colour was assumed to have an underlying SU(3) symmetry both baryons and mesons could be understood as colour neutral singlet states, which explains why colour was not seen before.

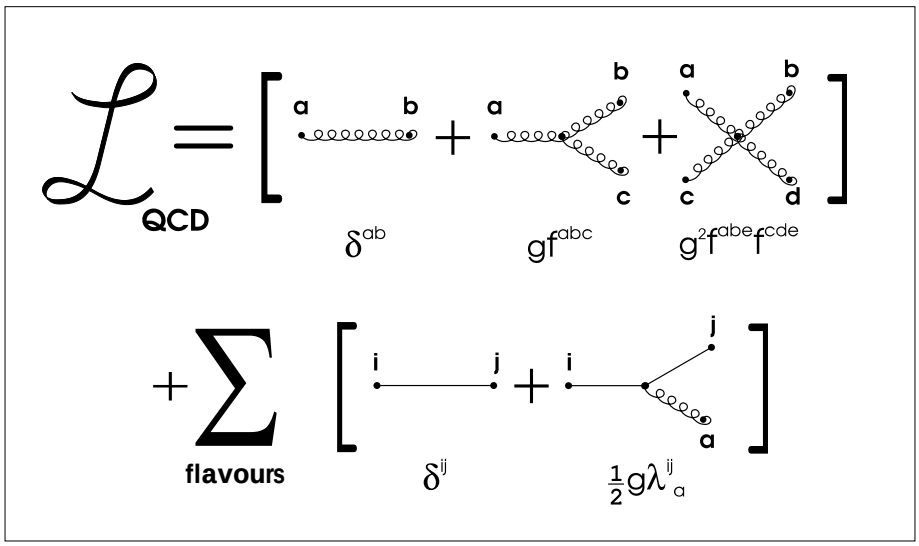

Figure 1: Pictorial representation of the QCD Lagrangian with the factors that determine the coupling strengths.

The ansatz that the colour degree of freedom constitutes the charge of a non–abelian gauge theory based on the gauge group SU(3) finally lead to the formulation of QCD [4] and a natural solution of the problems of the QPM. The gauge bosons of QCD, called gluons, are the invisible constituents of the nucleon and responsible for the strong interactions between the quarks observed through scaling violations. Also, the fact that free colour charges were never observed (see e.g. [5]) can be explained dynamically due to the fact that the potential between colour charges diverges with increasing distance [6]. An overview over the properties of QCD can be found e.g. in [3].

Up to gauge fixing terms, the Lagrangian of QCD, $\mathcal{L}_{\mathrm{QCD}}$, is the Yang-Mills Lagrangian for an unbroken SU(3) gauge symmetry, i.e. a theory with spin 1/2 fermions, massless spin 1

gauge bosons and one universal coupling constant $\alpha_s = g^2/4\pi$. Figure 1 gives a pictorial representation of $\mathcal{L}_{\rm QCD}$, showing the free fields and interaction terms together with the factors which determine the relative coupling strengths. Quarks have three and gluons have eight colour degrees of freedom. The amplitude for a quark changing its colour from i to j by emitting a gluon of type c is given by gT^c_{ji}, with the generators $T^c_{ji} = \lambda^c_{ji}/2$ proportional to the Gell-Mann matrices λ^c_{ji}. The amplitude for a gluon of type a changing to b by emitting a gluon of type c is given by gf^{abc}, with f^{abc} the structure constants of SU(3). The existence of the latter kind of coupling $f^{abc} \neq 0$ is characteristic for a non–abelian theory. Although the gauge symmetry is unbroken, the conceptually simple situation is complicated by the large value of the strong coupling constant which renders perturbative calculations reliable only in the limit of large momentum transfers.

2 Measurements of $\alpha_{\rm s}$

The QCD prediction for a cross section at an energy scale Q^2, evaluated in the $\overline{\rm MS}$ renormalization scheme, can be written in the form

$$\sigma(Q^2) = f(\alpha_s(\mu), Q^2) = \alpha_s(\mu)A + \alpha_s^2(\mu)(B + b_0 A \ln(\mu^2/s) + \mathcal{O}(\alpha_s^3). \qquad (1)$$

Here μ is the arbitrary renormalization point used in the calculation. For choices $\mu = Q$ the above expansion is a power series in $\alpha_s(\mu)$, for $|\ln(\mu^2/Q^2)| \gg 1$ it becomes an expansion in $\alpha_s(\mu)\ln(\mu^2/Q^2)$. In the latter case the expansion parameter can become large, thereby spoiling the convergence of the perturbative prediction. It follows, that a process with an intrinsic energy scale Q allows a measurement of the strong coupling at essentially the same scale.

The renormalization scale dependence of α_s is described by the beta function

$$\mu^2 \frac{d\alpha_s(\mu)}{d\mu^2} = -b_0 {\alpha_s}^2(\mu) + \mathcal{O}(\alpha_s^3) \quad \text{with} \quad b_0 = \frac{11C_A - 4T_F n_f}{12\pi}. \qquad (2)$$

For QCD one has $C_A = 3$ and $T_F = 1/2$. The quantity n_f is the number of active quark flavours. Using Eq.(2) measurements of α_s obtained at different energy scales can be compared, either by evolving backwards to the point Λ where α_s diverges, or by evolving to a common reference energy, which in recent years has become the Z mass.

2.1 Sum Rules

Measurements of the strong coupling constant based on sum rules represent fully inclusive measurements at a very low Q^2–scale. The theoretical prediction for the perturbative correction to the simple QPM is known to $\mathcal{O}(\alpha_s^3)$, together with some estimates of the non–perturbative ("higher twist") terms. Analyses exist based on the Bjorken sum rule (BJSR) [7] and the Gross-Llewellyn-Smith sum rules (GLSR) [8]. The results are given in Tab. 1 at the scale of the measurements and evolved up to the Z mass.

2.2 The Ratios R_Z, R_γ and R_τ

Another set of inclusive measurements of α_s, where the theoretical prediction is known to $\mathcal{O}(\alpha_s^3)$ is based on the ratios of the hadronic to leptonic branching ratios of the Z (R_Z), a virtual photon

Measurement	μ/GeV	$\alpha_s(\mu)$	$\alpha_s(M_Z)$
BJSR [7]	1.58	$0.375 \pm {}^{0.062}_{0.081}$	$0.122 \pm {}^{0.005}_{0.009}$
GLSR [8]	1.732	0.240 ± 0.047	$0.107 \pm {}^{0.007}_{0.009}$
R_Z [9, 10, 11]	91.2	0.128 ± 0.006	0.128 ± 0.006
R_γ [12]	31.6	0.153 ± 0.017	0.127 ± 0.012
R_γ [13]	34.0	0.165 ± 0.022	0.136 ± 0.015
R_τ [14]	1.777	0.375 ± 0.032	0.123 ± 0.003
R_τ [15]	1.777	0.302 ± 0.035	0.124 ± 0.004
R_τ, Moments [16]	1.777	0.355 ± 0.021	0.121 ± 0.003
R_τ(PDG), Moments [17]	1.777	$0.302 \pm {}^{0.024}_{0.025}$	0.114 ± 0.003
$\eta_c \to \gamma\gamma$ [17]	2.98	0.187 ± 0.029	0.101 ± 0.010
$\Gamma(\Upsilon \to gg\gamma)/\Gamma(\Upsilon \to ggg)$ [17]	9.46	0.164 ± 0.013	0.111 ± 0.006
$\Gamma(J/\Psi, \Upsilon \to ggg)/\Gamma(J/Psi, \Upsilon \to e^+e^-)$ [18]	10.0	$0.167 \pm {}^{0.015}_{0.011}$	$0.113 \pm {}^{0.007}_{0.005}$
Lattice Gauge Theory (Υ level splitting) [19]	5.0	0.203 ± 0.010	0.115 ± 0.002
Deep Inelastic Scattering	7.1	0.177 ± 0.012	0.113 ± 0.005
scaling violation in e^+e^--annihilation [20]	56.5		0.118 ± 0.005
scaling violation in e^+e^--annihilation [21]	44.7		0.127 ± 0.011
$ep \to$ Jets [22]	17.3		0.123 ± 0.018
$ep \to$ Jets [23]	20.4	$0.150 \pm {}^{0.014}_{0.013}$	0.126 ± 0.008
$p\bar{p} \to$ W+Jets [24]	80.2	0.123 ± 0.025	0.121 ± 0.024
$p\bar{p} \to$ W+Jets [25]	80.2	$0.123 \pm {}^{0.015}_{0.014}$	$0.120 \pm {}^{0.014}_{0.012}$
$pp, p\bar{p} \to \gamma$ +Jets [26]	4.0	$0.206 \pm {}^{0.042}_{0.033}$	$0.112 \pm {}^{0.012}_{0.010}$
$p\bar{p} -> b\bar{b}$+Jets [27]	20.0	$0.138 \pm {}^{0.028}_{0.019}$	$0.109 \pm {}^{0.016}_{0.012}$
$e^+e^- \to$ hadrons (event shapes) [28]	10.53	0.164 ± 0.015	0.113 ± 0.006
$e^+e^- \to$ hadrons (event shapes) [29]	29.0	0.160 ± 0.012	0.129 ± 0.008
$e^+e^- \to$ hadrons (event shapes) [30]	29.0	0.149 ± 0.007	0.122 ± 0.005
$e^+e^- \to$ hadrons (event shapes) [31]	34.0	0.140 ± 0.020	0.119 ± 0.014
$e^+e^- \to$ hadrons (event shapes) [32]	53.3	0.129 ± 0.012	0.119 ± 0.010
$e^+e^- \to$ hadrons (event shapes) [33]	57.9	0.134 ± 0.006	0.124 ± 0.005
$e^+e^- \to$ hadrons (event shapes) [34]	58.0	0.132 ± 0.005	0.123 ± 0.004
$e^+e^- \to$ hadrons (event shapes) [35]	58.0	0.139 ± 0.008	0.129 ± 0.007
$e^+e^- \to$ hadrons (event shapes) [36]	58.5	0.129 ± 0.006	0.120 ± 0.005
$e^+e^- \to$ hadrons (event shapes) [32]	59.5	0.122 ± 0.013	0.114 ± 0.012
$e^+e^- \to$ hadrons (event shapes) [30]	91.2	0.123 ± 0.010	0.123 ± 0.010
$e^+e^- \to$ hadrons (event shapes) [37]	91.2	0.120 ± 0.008	0.120 ± 0.008
$e^+e^- \to$ hadrons (event shapes) [38]	91.2	0.125 ± 0.005	0.125 ± 0.005
$e^+e^- \to$ hadrons (event shapes) [39]	91.2	0.123 ± 0.006	0.123 ± 0.006
$e^+e^- \to$ hadrons (event shapes) [40]	91.2	0.124 ± 0.007	0.124 ± 0.007
$e^+e^- \to$ hadrons (event shapes) [41]	91.2	0.120 ± 0.006	0.120 ± 0.006

Table 1: Compilation of measurements of the strong coupling constant. The errors are the total uncertainties, which in most cases are dominated by the theoretical uncertainties.

(R_γ) or the tau-lepton (R_τ). In all cases the hadronic system is formed from the electroweak (EW) coupling of a vector boson (Z, Photon or W) to a primary quark-antiquark pair. The sensitivity to the strong coupling comes about from gluon radiation off the primary quarks. This radiation opens up new final states for the hadronic system which increase the hadronic width with respect to the purely electroweak expectation. The theoretical prediction can be organized in the following form:

$$R_{Z,\gamma,\tau} = R^{EW}_{Z,\gamma,\tau}(1 + \delta_{QCD} + \delta_m + \delta_{np}) \tag{3}$$

Here δ_{QCD} is the perturbative QCD correction for massless quarks, which in all cases dominates the correction, δ_m is an additional correction due to finite quark masses, and δ_{np} the impact of non–perturbative effects, which is small for all three observables.

A simple effective parametrization to translate a measurement of R_Z into a corresponding value $\alpha_s(M_Z)$ together with an estimate for the theoretical uncertainties is given in [10]. Using the combined result from LEP [9], $R_Z = 20.800 \pm 0.035$ and the latest direct measurement of the top mass [11], one obtains $\alpha_s(M_Z) = 0.128 \pm 0.005(\mathrm{stat}) \pm 0.003(\mathrm{EW}) \pm 0.002(\mathrm{QCD})$. Here the purely statistical error still dominates the total uncertainty, followed by the uncertainties related to the electroweak sector with equal contributions from the errors of top-quark and Higgs mass and the treatment of the radiative corrections. The genuine QCD uncertainties are smallest.

Results from R_γ are published in [12, 13] based on measurements from e^+e^-–annihilations into hadrons with centre–of–mass energies up to 56 GeV. Both analyses were still using the erroneous third order term $+64(\alpha_s/\pi)^3$ [42] instead of $-12.8(\alpha_s/\pi)^3$ [43] and are slightly biased due to the fact that the electroweak parameters were different from the values as they are known today. The published values corrected for the wrong third order coefficient are given in Tab. 1. The corrected results are consistent with a recent reanalysis [44] $\alpha_s(M_Z) = 0.128 \pm^{0.012}_{0.013}$.

For the determination of alphas from R_τ [45, 46] a good understanding of the non–perturbative terms is essential, which are potentially large as a consequence of the low energy scale and the correspondingly large value of α_s. The purely perturbative expansion is converging rapidly due to the fact that the integration over the hadronic mass spectrum from tau decays yields the observable double inclusive: integrated over all final state at a fixed mass of the hadronic system and integrated over all masses between m_π and M_τ.

Non–perturbative contributions can be treated in the framework of the SVZ approach [47], which allows to parametrize non–perturbative effects as power law corrections proportional to universal vacuum expectation values (condensates) of the QCD fields. Given that theses condensates not only affect R_τ but also all moments of the hadronic mass spectrum, they can be extracted from a simultaneous analysis of R_τ and sets of moments of the mass spectrum [46]. It turns out that the non–perturbative correction are surprisingly small, which implies that an α_s measurement based on R_τ is very accurate. There are however arguments [48], that the smallness of the non–perturbative effects is due to an accidental cancellation or that the SVZ–ansatz is invalidated by renormalon effects. In this case, the uncertainties would be significantly underestimated.

A measurement of α_s based on R_τ is available from the OPAL Collaboration [14]. Similarly, but combining information from different experiments, other measurements of R_τ and α_s are obtained from the leptonic branching ratios of the tau and the relation between tau mass and lifetime. Assuming the validity of the completeness relation for the tau branching ratios into hadrons, electrons and muons, $B_{\mathrm{hadr}} + B_e + B_\mu = 1$, the ratio R_τ can be expressed as function

of B_e

$$R_\tau = \frac{1 - B_e - B_\mu}{B_e} = \frac{1}{B_e} - 1 - f_\mu. \tag{4}$$

The factor $f_\mu = B_\mu/B_e = 0.9726$ takes into account that the muon decay is slightly suppressed due to the larger mass of the muon. Using the calculated value for f_μ as input, two independent determinations of R_τ are obtained from measurements of B_e and $B_\mu = B_e f_\mu$. A third result for R_τ via B_e can be obtained from a comparison of the masses and lifetime of the tau lepton and the muon. The standard model predicts

$$\frac{\Gamma_e(\mu)}{\Gamma_e(\tau)} = \frac{\Gamma_{tot}(\mu)}{B_e \Gamma_{tot}(\tau)} = \frac{m_\mu^5}{m_\tau^5} \quad \Rightarrow \quad B_e = \frac{\tau_\tau}{\tau_\mu} \left(\frac{m_\tau}{m_\mu}\right)^5. \tag{5}$$

With the numbers available before this conference [15] $m_\tau = 1777.0 \pm 0.3$ MeV/c^2, $\tau_\tau = 291.44 \pm 1.73$ fs, $B_e = 0.17787 \pm 0.00087$ and $B_\mu = 0.17332 \pm 0.00087$ one obtains the combined result $R_\tau = 3.641 \pm 0.017$. An α_s-measurement based on this value for R_τ with the condensates taken from [45] and the evolution to the scale of the Z mass done according to [49] is also given in Tab. 1. The error is almost entirely due to theoretical uncertainties.

Results based on R_τ and the leading moments of the hadronic mass spectrum are published by ALEPH [16] and CLEO [17] (see Tab. 1). The slight discrepancy between the two analyses can be traced to the determination of R_τ, which in the case of ALEPH is based on the measurements of the leptonic branching ratios done by the same collaboration, whereas the CLEO Collaboration uses the current PDG–values. The moments extracted from the hadronic mass spectrum are in good agreement.

2.3 Heavy Quarkonia

Various determinations of the strong coupling constant exist from studies of heavy quarkonia. Two new (preliminary) measurements were presented by the CLEO collaboration [17], based on branching ratios of the η_c and the Υ. The first measurement is based on the partial width $\Gamma(\eta_c \to \gamma\gamma)$ measured in two–photon processes, the second one on the ratio $\Gamma(\Upsilon \to gg\gamma)/\Gamma(\Upsilon \to ggg)$, which is proportional to α_{em}/α_s. The results from both analyses are given in Tab. 1.

Another measurement is derived from the ratio of the hadronic to the leptonic width of a heavy quark–antiquark pair. To leading order this ratio, understood as the annihilation into three gluons compared to the annihilation into a lepton pair, is proportional to α_s^3/α_{em}^2. A combined analysis of this ratio from Υ and J/Ψ decays allows a simultaneous determination of α_s and the size of the non–perturbative effects due to relativistic corrections in the bound state system [18]. Assuming that those effects are proportional to the average $< v^2/c^2 >$ of the quarks, the theoretical prediction, which is known to next–to–leading order can be parametrized as

$$\frac{\Gamma(q\bar{q} \to hadrons)}{\Gamma(q\bar{q} \to e^+e^-)} = \frac{\alpha_s^3}{\alpha_{em}^2}(A + B\alpha_s + C{\alpha_s}^2) \left(1 + D \left\langle \frac{v^2}{c^2} \right\rangle\right). \tag{6}$$

The coefficients A and B are known from perturbative QCD, C is a higher order term that is varied to probe the theoretical uncertainties of the perturbative prediction, and D is a free parameter to take into account relativistic corrections for the bound state system. The free parameters in a combined analysis of the Υ and the J/Ψ are α_s and D. The results, at the scale of the measurement and evolved up to the Z mass is given in Tab. 1. The error is dominated by the theoretical uncertainties.

2.4 Lattice Gauge Theories

Rather precise determinations of α_s derived from lattice gauge theories are becoming available from the analysis of level splittings between the S– and the P–states in the Υ–system [19]. Calculations exist with $n_f = 0$ and $n_f = 2$ dynamic fermion generations, i.e. fermions in loop corrections, which give only marginally different results and thus allow a safe extrapolation to the physical case of $n_f = 3$ light flavours. The result is given in Tab. 1. A crucial point of the analysis is the conversion form the lattice coupling to the $\overline{\rm MS}$ coupling constant used elsewhere. Initially large discrepancies between the lattice results and other measurements could be traced to imprecisions in this conversion.

2.5 Scaling Violations

Measurements of the strong coupling constant exist from the analysis of scaling violations in structure functions of the nucleon, i.e. space–like momentum transfers $Q^2 = -t$, and in the time–like domain $Q^2 = s$ from the study of fragmentation functions in e^+e^--annihilations. In both cases the scale breaking is described by Dokshitzer–Gribov–Lipatov–Altarelli–Parisi (DGLAP) [58] evolution equations, which predict a softening $d\ln F(x,Q^2)/d\ln Q^2$ proportional to α_s with increasing Q^2. For structure functions the softening comes about because higher momentum transfers resolve more partons from vacuum fluctuations in the nucleon, for fragmentation functions the enlarged phase space permits additional gluon radiation and particle production with a probability proportional α_s. The theory is known to next–to–leading order [59, 60]. A measurement of the strong coupling constant based on scaling violations allows a simultaneous determination of the non–perturbative effects, which manifest themselves as power law correction to the logarithmic QCD effects. The different Q^2–dependence allows to disentangle the two contributions. In this respect measurements from Deep Inelastic Scattering (DIS) processes are favoured because here the power law corrections are known to decrease rapidly with $1/Q^2$. For the case of e^+e^--annihilation processes there are arguments that they decay only proportional to $1/Q$ [60]. As a consequence, here the dynamic range available to disentangle the effects of perturbative and non–perturbative QCD when comparing measurements between $\sqrt{s} = 22$ GeV and $\sqrt{s} = 91.2$ GeV is much smaller than the one available for the DIS-measurements, which typically cover a range between $Q^2 = 0.5$ GeV^2 and $Q^2 = 260$ GeV^2 [53].

Measurements of the strong coupling constant in DIS exist from lepton–nucleon scattering experiments with neutrino, electron and muon beams. Using charged leptons, values for $\Lambda^{(4)}_{\overline{\rm MS}}$ are published by the BCDMS [50] and EMC [51]/NMC [52] collaboration and in a combined analysis of SLAC and BCDMS data [53]. Results from neutrino beams are given by the CHARM [54], CDHSW [55] and the CCFR [56] collaboration. All numbers in good agreement. The average quoted below uses the re–analyzed CDHSW result as presented and discussed in detail in reference [57]. The weighted average considering only the experimental errors is $\Lambda^{(4)}_{\overline{\rm MS}} = 245 \pm 26$ MeV, with a $\chi^2/{\rm df} = 2.6/6$. The individual measurements are shown in Fig. 2. Assuming that the theoretical uncertainties determined in [53] apply throughout, one obtains the result listed in Tab. 1. The error is dominated by the theoretical uncertainties.

A first results from the analysis of scaling violations in fragmentation functions was published by the DELPHI collaboration [20]. The theoretical prediction was determined by the LUND matrix element model with the cutoff of the perturbative phase held at a fixed mass. Using a complete Monte Carlo model which combines fixed second order perturbative QCD with non–perturbative effects leaves only a small number of free parameters in addition to $\alpha_s(M_Z)$.

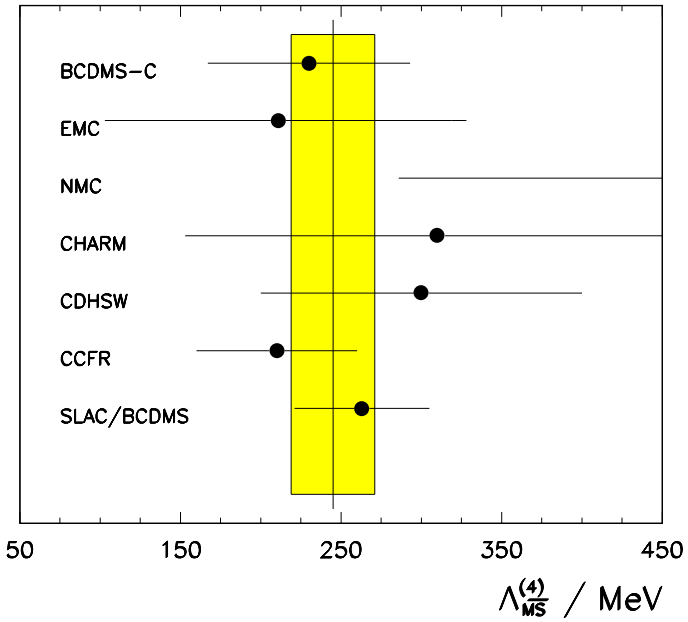

Reference	$\Lambda^{(4)}_{\overline{MS}}$/MeV
BCDMS [50]	230 ± 63
EMC [51]	$211 \pm {}^{117}_{108}$
NMC [52]	838 ± 552
CHARM [54]	310 ± 157
CDHSW [57]	300 ± 100
CCFR [56]	210 ± 50
SLAC/BCDMS [53]	263 ± 42
Average	245 ± 26

Figure 2: Measurements of $\Lambda^{(4)}_{\overline{MS}}$ from DIS. The errors are the purely experimental errors.

From this a precise measurement of the strong coupling constant $\alpha_s(M_Z) = 0.118 \pm 0.005$ was obtained, in good agreement with other determinations. A measurement based on the exact NLO theoretical framework without using information from a Monte Carlo model was later presented by the ALEPH Collaboration [21]. Here not only the strong coupling constant, but also parametrizations for the fragmentation functions of all quark flavours and the gluon together with the energy dependence of the non–perturbative effects were extracted from the data. The result of this model independent analysis was $\alpha_s(M_Z) = 0.127 \pm 0.011$. The final result published recently is $\alpha_s(M_Z) = 0.126 \pm 0.009$ [61]. The larger error is due to the fact, that the analysis is based only on experimental data without relying on Monte Carlo predictions. A comparison between the data and the QCD fit is shown in Fig. 3, together with the amount of scaling violations observed in fragmentation functions when varying the centre-of-mass energy from $\sqrt{s} = 22$ GeV to $\sqrt{s} = 91.2$ GeV.

2.6 Processes with Jets

Various measurements of the strong coupling constant exploit the fact, that partons emitted in hard scattering processes which can be described by perturbative QCD, manifest themselves as jets of hadrons in the detector. The following subsections give an overview over results from those kinds of measurements.

Jet Production in *ep*-scattering

In *ep*-collisions the basic mechanism of jet production is the photon–gluon fusion process, where a large Q^2 virtual photon from the electron merges with a gluon from the struck proton to produce a quark–antiquark system. Alternatively the photon can merges with a quark from the proton to produce a final state quark-gluon system. Those two partons emerge as two jets in the detector in addition to the jet from the proton remnant. The production rate R_{2+1}

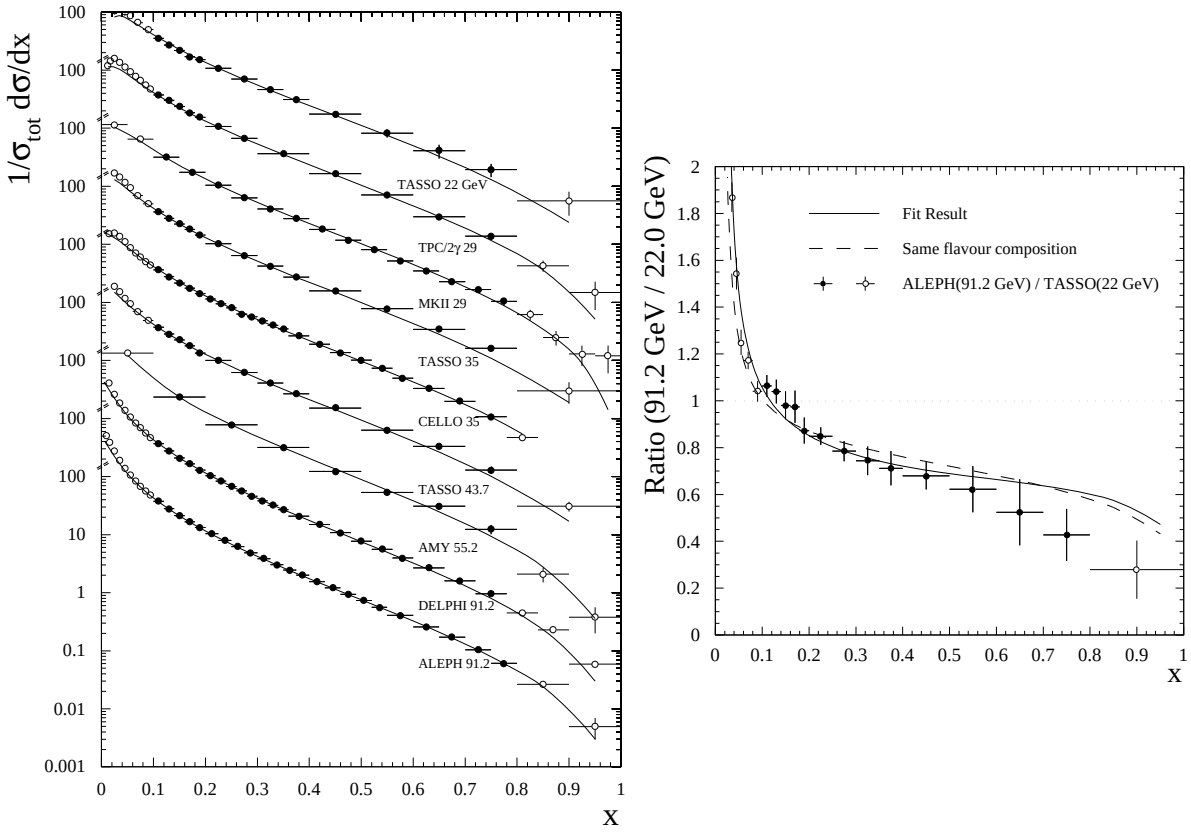

Figure 3: The left hand figure shows the inclusive cross sections for charged particles as function of the scaled momentum $x = 2p/\sqrt{s}$ for centre-of-mass energies between $\sqrt{s} = 22$ GeV and $\sqrt{s} = 91.2$ GeV. The lines are the result of a global QCD fit to these distributions together with flavour tagged samples from hadronic Z decays (not shown). The full dots were used in the fit. On the right hand the ratio between the cross sections at 22 GeV and 91.2 GeV is displayed. The full line is the result of the global QCD fit. For comparison also the prediction for constant flavour composition is shown.

of those final states is known to next-to-leading order $\mathcal{O}(\alpha_s^2)$. The appealing feature of this measurement is the fact, that by tagging the scattered electron it is possible to study the Q^2-dependence of the process, allowing to establish the running of the strong coupling constant within one experiment. First results from the Zeus [23] and the H1 [22] collaborations are listed in Tab. 1 and shown in Fig. 4.

Proton-Antiproton Annihilation into W+Jets

The strong coupling constant can also be determined from QCD-radiative corrections to the quark–antiquark fusion into a W. Also here the perturbative QCD-corrections are known to next–to–leading order $\mathcal{O}(\alpha_s^2)$. Measurements published by the UA2 [24] and D0 [25] collaborations can be found in Tab. 1.

Prompt Photon Production

The leading order diagrams for this kind of process are obtained from the diagrams for QCD–compton scattering or quark–antiquark annihilation into two gluons by replacing one of the

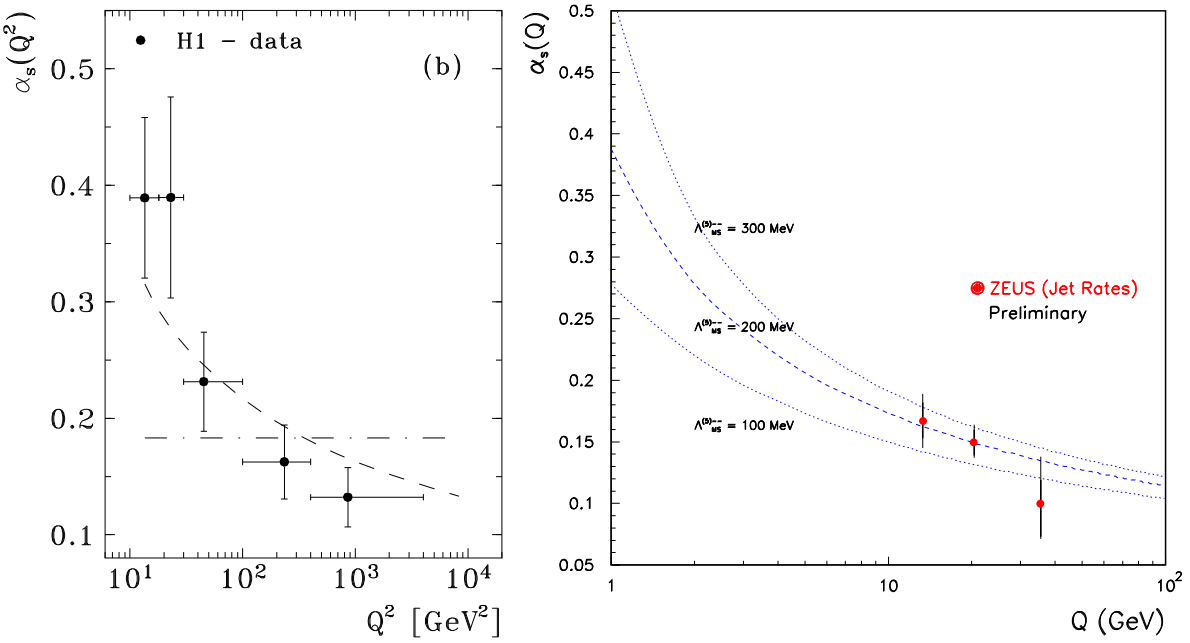

Figure 4: Measurements of strong coupling constant by the H1 and ZEUS collaborations.

gluons by a photon. The theoretical prediction thus is of $\mathcal{O}(\alpha_s\alpha_{em})$. A precise measurement of the strong coupling constant is possible by studying the difference $\sigma(p\overline{p}\rightarrow\gamma X) - \sigma(pp\rightarrow\gamma X)$ where the sea quark and gluon structure functions of the nucleon cancel. The difference depends only on the rather well measured valence quark distribution and α_s. The result corresponding to a measurement [26] of the QCD scale $\Lambda^{(4)}_{\overline{\rm MS}} = 235 \pm 106^{+146}_{-9}$ MeV done at the typical scale $Q = P_T = 4$ GeV is given in Tab. 1.

Heavy Quark Production in Proton-Antiproton Collisions

Heavy quarks which are not present in the initial state are produced by quark–antiquark annihilation or gluon–gluon fusion processes. Experimentally those reactions can be tagged by the decay characteristics of the heavy hadrons, which allows a measurement of the strong coupling. The result from an analysis of $b\overline{b}$+jets production in $p\bar{p}$ collisions [27] is given in Tab. 1.

2.7 Global Event Shape Variables

Measurements of α_s from global event shape variables are the domain of e^+e^--annihilation experiments into quark-antiquark pairs. Those primary quarks start emitting gluons, which in turn can split into secondary gluons or new quark-antiquark pairs. This parton showering process proceeds until the virtuality of the partons is around 1 GeV, where the non–perturbative hadronization process takes over and the final state hadrons are formed. An important feature of the parton shower is "angular ordering", i.e. decreasing emission angles of secondary partons in the shower. Thus the momentum flow is collimated in the direction of the primary quarks, explaining the two-jet structure of most hadronic events. If a hard gluon is emitted at large angle in the initial phase of the parton shower, three distinct jets are formed. Angular ordering

thus provides a perturbative explanation for the interpretation of jets as the hard partonic skeleton of an event.

A measurement of the strong coupling constant from event shape variables is based on the idea that to leading order the ratio of the 3-jet and the 2-jet cross section is proportional to α_s. To exploit this concept one needs to define variables which are sensitive to the topology of multijet events. Those variables have to be "infrared" and "collinear" safe in order to be calculable in perturbation theory, i.e. they must not change in the limit that the energy of an additional soft gluon goes to zero or if any of the final state momenta is split into two collinear ones.

Many observables satisfying the above criteria have been defined. Central to various subsequent definitions is *thrust* T [62], which measures the collimation of the momentum flow in an event:

$$T = \max_{|\vec{n}|=1} \frac{\sum_p |\vec{p}\cdot\vec{n}|}{\sum_p |\vec{p}|} \tag{7}$$

An ideal 2–jet event has $T = 1$, a perfectly isotropic one has $T = 1/2$. The thrust axis $\vec{n}$ is the direction along which the momentum flow is maximal. It thus defines a natural event axis and is a good estimator for the direction of flight of the initial quark–antiquark pair. Given the thrust axis, the event can be divided into two hemispheres by the plane orthogonal to $\vec{n}$. The invariant masses of the two hemispheres, M_H being the larger and M_L the smaller one, then allow two define two new event shape variables [63]: *heavy-jet mass* $\rho = M_H^2/s$ and *mass difference* $m_d^2 = (M_H^2 - M_L^2)/s$.

Another common variable is y_3, derived from the measurement of jet rates by means of a clustering algorithm. Here the 4-momenta of the final state particles are recombined into jets in an iterative procedure. The algorithm starts by considering each particle to be a jet. Then those two jets with 4–momenta p_i and p_j which are closest in phase space e.g. according to the Durham–metric [64], $y_{ik} = 2\min(E_i^2, E_j^2)(1-\cos\theta_{ij})/s$, are combined by adding their 4-momenta ("E–scheme"). Iterating the procedure until only three pseudo-particles ("jets") are left, y_3 is defined by $y_3 = \min(y_{12}, y_{23}, y_{31})$. For a further discussion see for example [65].

According to general theorems [66] the perturbative prediction for the cumulative cross section of any event shape variable X, which vanishes in the limit of perfect 2-jet topologies, can be expressed in the form

$$R(L) \equiv \frac{\sigma(-\ln(X) > L)}{\sigma_{tot}} = \left(1 + \sum_{i=1}^{\infty} C_i \alpha_s^i\right) \exp\left(\sum_{n=1}^{\infty}\sum_{m=1}^{2n} G_{nm}\alpha_s^n L^m\right) + \sum_{k=1}^{\infty} \alpha_s^k D_k(L).$$

The $D_k(L)$ are regular functions which vanish in the limit $L \to \infty$. For the special case that the perturbative prediction exponentiates one gets a simplified expression with $G_{nm} = 0$ for $m > n+1$. In this case the terms of perturbative prediction for $\ln R$ can be organized as follows:

LL	NLL	Subleading Terms			
$\alpha_s L^2$	$\alpha_s L$	α_s	$\alpha_s S_1(L)$		
$\alpha_s^2 L^3$	$\alpha_s^2 L^2$	$\alpha_s^2 L$	α_s^2	$\alpha_s^2 S_2(L)$	
$\alpha_s^3 L^4$	$\alpha_s^3 L^3$	$\alpha_s^3 L^2$	$\alpha_s^3 L$	α_s^3	$\alpha_s^3 S_3(L)$
$\alpha_s^4 L^5$	$\alpha_s^4 L^4$	$\alpha_s^4 L^3$	$\cdots$		
$\vdots$	$\vdots$	$\vdots$	$\ddots$		

The first two columns are the leading– and next–to–leading logarithms, which for some event shape variables have been resummed into analytic functions $LG_{LL}(\alpha_s L)$ and $G_{NLL}(\alpha_s L)$. Examples are $\tau = 1 - T$ and ρ. The functions $S_k(L)$ are combinations of the $D_k(L)$ and the coefficients C_i. They also vanish for $L \to \infty$. The first two rows constitute the theoretical prediction in second order perturbation theory. Based on numerical integration [67] of the ERT-matrix elements [68] the corresponding expressions are known for all event shape variables.

If the second order and the leading– plus next–to–leading-log resummed predictions both are available, an improved theoretical prediction is obtained by combining the two, which is exact to $\mathcal{O}(\alpha_s^2)$ over the whole phase space and contains the dominant terms to all orders in the vicinity of the 2–jet region ($X \to 0$). There is a certain freedom in performing the matching of the theoretical predictions [69] which can be employed to probe the sensitivity of an α_s measurement to the unknown higher order corrections. Typical examples are the so called $\ln R$-matching and the R-matching schemes, where the predictions for R or $\ln R$ are combined. The results differ in $\mathcal{O}(\alpha_s^3)$. Another way to assess theoretical uncertainties is the variation of the renormalization scale, i.e. doing a measurement of $\alpha_s(\mu)$ instead of $\alpha_s(Q)$. Also here, when based on an the full $\mathcal{O}(\alpha_s^2)$–prediction, the change in $\alpha_s(M_Z)$ is of $\mathcal{O}(\alpha_s^3)$, the first uncalculated higher order corrections. For a complete perturbative prediction there would be no renormalization scale dependence. Other ways to estimate the theoretical uncertainties of a perturbative prediction exist. Examples can be found in [16, 18, 70]. As a safeguard against accidental cancellations usually several methods are combined in order to assess the error due to unknown higher order perturbative effects.

Another class of theoretical uncertainties outside the domain of perturbative QCD is related to the hadronization process. For α_s–measurements based on event shape variables the estimates of size and uncertainty of non–perturbative effects so far rely on Monte Carlo models [71]. Results from α_s–determinations based on global event shape variables done at centre–of–mass energies between $\sqrt{s} = 10.53$ GeV and $\sqrt{s} = 91.2$ GeV are listed in Tab. 1. Where available, the numbers are single experiment averages over various event shape variables. For more detailed information see e.g. [72].

2.8 Combination of Individual Results

Measurements of the strong coupling constant are available from a multitude of reactions, with error estimates based on a careful evaluation of the statistical errors, the experimental systematics and the theoretical uncertainties. Being the dominant errors in α_s–measurements, the latter deserve some further discussion.

Problems arise, because there is no general consensus how to determine the theoretical uncertainties. As a consequence subjective judgement has to be used to determine errors which correspond to 68% confidence level intervals. Based on some experience about how errors behave those estimates will on average be reliable, even if individual numbers are somewhere between too optimistic and too pessimistic. The non–statistical nature of theoretical errors implies, that they must be viewed as a Bayesian estimates parametrizing the knowledge gained in a measurement. Interpreting also the experimental errors this way then can be taken as a justification to combine experimental and theoretical errors in quadrature.

Another point of concern is the fact, that theoretical errors in different measurements are correlated. The best way to deal with those correlations would be to give the derivatives of the result with respect to the various sources of uncertainty. Instead in many cases only the total

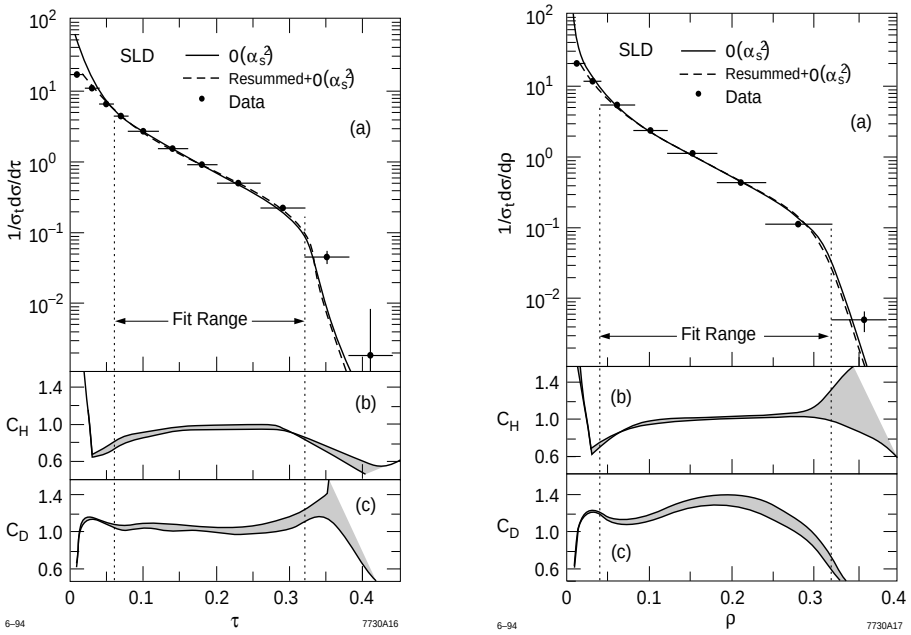

Figure 5: Examples for measurements of α_s based on global event shape variables. The distributions compared to the QCD fits are shown in (a). In (b) the size and uncertainties for the hadronization corrections are displayed and in (c) the same information is given for the detector corrections.

error is given, leading to a situation where measurements are known to be correlated with very little information about the actual size of those correlations.

A proposal how to average such measurements is given in [73]. An optimal average which minimizes the variance of combined result is not feasible if the correlations cannot be reliably reconstructed. The latter would require a breakdown of the single uncertainties along the lines described above. Instead a standard weighted average is formed, with weights given by the inverse of the single variances.

$$\bar{x} = \sum_{i=1}^{n} w_i x_i \quad \text{with} \quad w_i \sim \frac{1}{\sigma_i^2} \quad \text{and} \quad \sum_{i=1}^{n} w_i = 1. \tag{8}$$

This is a robust estimate which is also optimal if the single measurements are uncorrelated. The error of the average is given by

$$\sigma^2(\bar{x}) = \sum_{i,j=1}^{n} w_i w_j C_{ij} \tag{9}$$

where C_{ij} is the covariance matrix of the measurements. In order to determine $\sigma^2(\bar{x})$ one has to know the full covariance matrix or at least an effective parametrization of it. The proposal [73] uses the latter approach, making the ansatz

$$C_{ij} = \begin{cases} \sigma_i^2 & i = j \\ \rho \sigma_i \sigma_j & i \neq j \end{cases} \tag{10}$$

Information about the unknown effective correlation-coefficient ρ can be obtained from the χ^2 of the average

$$\chi^2 = \sum_{i,j=1}^{n} (x_i - \bar{x})(x_j - \bar{x}) C_{ij}^{-1}. \tag{11}$$

With $\bar{x}$ defined according to Eq.(8) the expectation value of this quantity is $< \chi^2 >= n-1 \equiv N_{df} = n-1$ for $\rho = 0$. Negative correlations would lead to $\chi^2 > N_{df}$, positive ones to $\chi^2 < N_{df}$. In the former case an error estimate based on the assumption $\rho = 0$ would overestimate the true uncertainty, in the latter it would underestimate it. The same behaviour would be observed if the individual errors are underestimated ($\chi^2 > N_{df}$) or overestimated ($\chi^2 < N_{df}$). For the case $\chi^2 > N_{df}$ the PDG has adopted the practice to conservatively assume that the errors are underestimated by a common factor $S = \sqrt{\chi^2/N_{df}}$ and to scale the error of the average correspondingly. In [73] the proposal is made to interpret a $\chi^2 < N_{df}$ as evidence for the existence of positive correlations, to determine a parameter ρ such that $\chi^2 = N_{df}$ and to use this value ρ in the error calculation for the average based on Eq.(9). Both procedures conservatively interpret any deviation of χ^2 from its expectation value as evidence for having underestimated the error of the average and invoke an appropriate scaling scheme.

The properties of the proposed procedure can be illustrated by considering two measurements x_1 and x_2 which have the same error σ. One obtains $\bar{x} = (x_1 + x_2)/2$, $\chi^2 = (x_1 - x_2)^2/2\sigma^2$ and $\sigma^2(\bar{x}) = \sigma^2(1 - \chi^2/2)$ for $\chi^2 < 1$. In the limiting case $x_1 = x_2$ averaging does not decrease the error. In general one finds that averaging highly correlated data with this procedure leads to an average of the measurements and the errors, which is perfectly appropriate when individual error estimates to some extent are based on subjective judgement

Averages determined according to the procedure described above [73] will be referred to as "correlated averages" in the following.

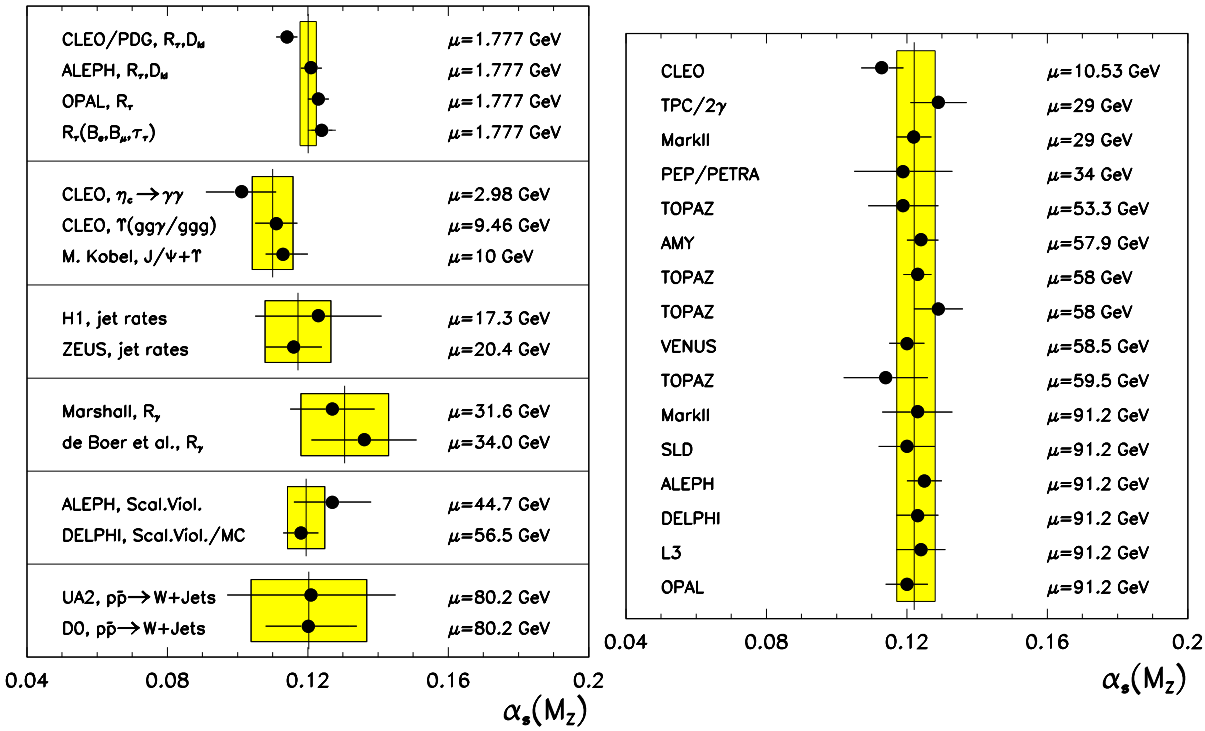

Figure 6: Overview over different types of α_s–measurements. The shaded boxes are the correlated averages (see text) for the respective groups.

Figure 6 gives an overview over the different types of α_s–measurements together with their correlated averages. On the right hand side of α_s–determinations based on global event shape

Measurement	μ/GeV	$\alpha_s(\mu)$	$\alpha_s(M_Z)$
BJSR	1.58	$0.375 \pm {}^{0.062}_{0.081}$	$0.122 \pm {}^{0.005}_{0.009}$
GLSR	1.732	0.240 ± 0.047	$0.107 \pm {}^{0.007}_{0.009}$
R_τ	1.777	$0.330 \pm {}^{0.019}_{0.018}$	0.1201 ± 0.0023
$pp, p\bar{p} \rightarrow \gamma$ +Jets	4.0	$0.206 \pm {}^{0.042}_{0.033}$	$0.112 \pm {}^{0.012}_{0.010}$
Lattice Gauge Theory	5.0	0.203 ± 0.010	0.115 ± 0.002
Deep Inelastic Scattering	7.1	0.177 ± 0.012	0.113 ± 0.005
Heavy Quarkonia	2.98	0.187 ± 0.029	0.101 ± 0.010
$ep \rightarrow$ Jets	18.	$0.155 \pm {}^{0.017}_{0.016}$	0.117 ± 0.009
$p\bar{p} -> b\bar{b}$+Jets	20.0	$0.138 \pm {}^{0.028}_{0.019}$	$0.109 \pm {}^{0.016}_{0.012}$
R_γ	33.	$0.157 \pm {}^{0.019}_{0.018}$	0.1305 ± 0.0125
scaling violation in e^+e^--annihilation	50.	$0.132 \pm {}^{0.007}_{0.006}$	0.1195 ± 0.0053
$e^+e^- \rightarrow$ hadrons (event shapes)	60.	0.131 ± 0.006	0.1221 ± 0.0050
$p\bar{p} \rightarrow$ W+Jets	80.2	0.123 ± 0.017	0.1203 ± 0.0165
R_Z	91.2	0.128 ± 0.006	0.128 ± 0.006

Table 2: Compilation of measurements of the strong coupling constant. The errors are the total uncertainties, which in most cases are dominated by the theoretical uncertainties.

variables are displayed. The correlated average is $\alpha_s(M_Z) = 0.122 \pm 0.005$. The unscaled error is $\Delta\alpha_s = 0.0016$ with a $\chi^2/N_{df} = 5.6/15$.

2.9 A Global Average

A summary of the various types of measurements as function of the typical scale and evolved up to the scale of the Z mass is listed in Tab. 2 and shown in Fig. 7. Since the running of the strong coupling to leading order is proportional to $1/\ln Q^2$, the geometric mean is quoted as the scale of the measurement when results from different scales were averaged. The running of the strong coupling constant consistent with the expectation from QCD is evident. The results are in good agreement with the current PDG average [74] $\alpha_s(M_Z) = 0.117 \pm 0.005$.

Doing a simple weighted average of the results given in Tab. 2 yields $\alpha_s(M_Z) = 0.1174 \pm 0.0012$ with $\chi^2/N_{df} = 12.6/13$. Although maybe defendable, this error estimate appears to be too optimistic, because a justification based on the χ^2-value gets its legitimation from the fact that some measurements are much less precise than others. Looking closer one sees that the measurements fall into two groups which scatter much less around a common value, indicating that there are common systematics. Combining low and high values separately one obtains the correlated averages $\alpha_s(M_Z) = 0.1212 \pm 0.0034$ and $\alpha_s(M_Z) = 0.1140 \pm 0.0032$ The correlated average of these two results is $\alpha_s(M_Z) = 0.1174 \pm 0.0036$, suggesting a new "world average" $\alpha_s(M_Z) = 0.117 \pm 0.004$ with a slightly smaller error than the current PDG value [74].

3 Tests of the Structure of QCD

Testing the structure of QCD means verifying that the partons carry the quantum numbers assigned to them according to the QCD Lagrangian. This program comprises the verification

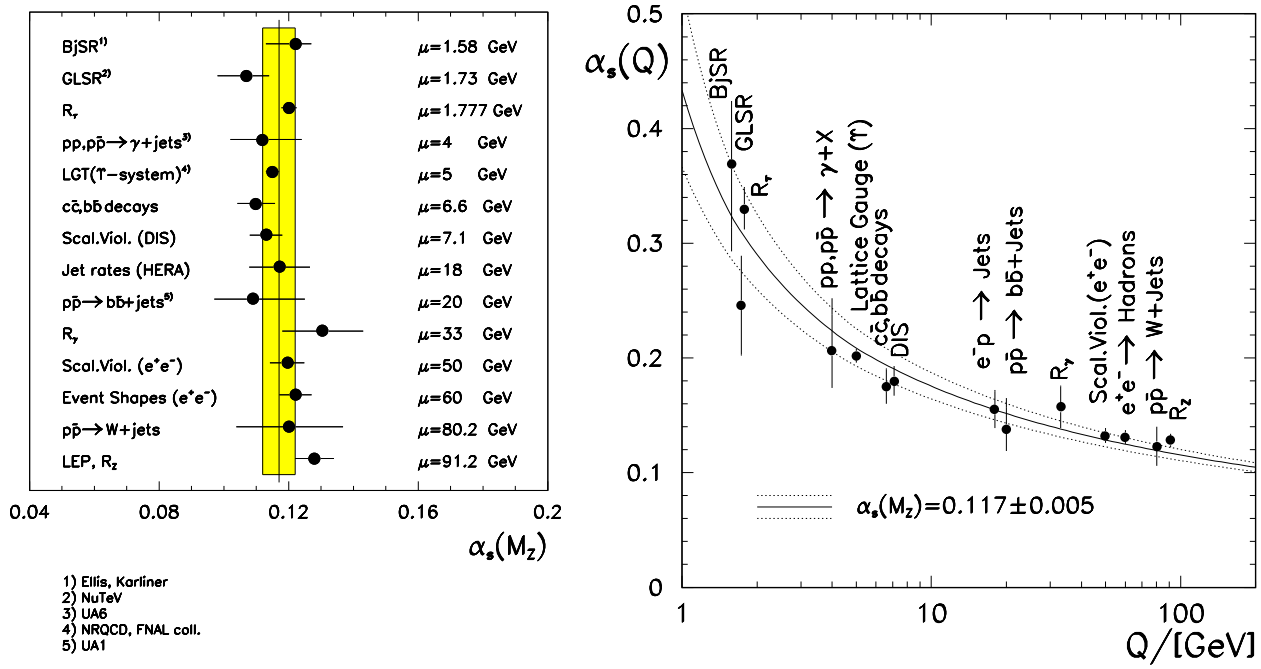

Figure 7: Overview over different types of α_s-measurements compared to the 1994 PDG average.

of the spin assignment for the partons, measurement of the colour charges of quarks and gluons and the test that colour charge of the quark is flavour independent.

3.1 Parton Spins

The spin of the quarks can be probed by studying the angular distribution of the thrust axis in e^+e^-–annihilation events into hadrons [75]. The thrust axis is a rather reliable measure of the direction of the initial partons since, as a consequence of angular ordering in the parton shower, the momentum flow remains collimated around the direction of the original partons. From angular momentum considerations one expects a distribution $1+\cos^2\Theta$ for two spin 1/2 fermions originating from the decay of a spin 1 particle (Z). Here Θ denotes the angle to the beam direction. Figure 8 shows the uncorrected angular distribution of the thrust axis seen in the ALPEH detector compared to a Monte Carlo calculation which includes the full detector simulation. The data are in perfect agreement with the spin 1/2 assignment for the quarks. The sensitivity to the quark spin is illustrated by comparing the measurements to the expectation for spin 0, which is clearly excluded.

The gluon spin can be inferred from the study of the kinematics in 3–jet event [76]. Published results can be found in [77]. The conceptually simplest measurement is obtained from the scaled energy distribution of the lowest energy jet in a 3–jet event, $d\sigma/dx_3$, with $x_3 = E_{jet}/E_{Beam}$. In the limit $x_3 \to 0$ one expects a double (infrared and collinear) singularity $d\sigma/dx_3 \sim x_3^{-2}$ for a vector gluon. For a scalar gluon, due to its helicity non–conserving coupling to the fermion current, only the collinear singularity exists, i.e. $d\sigma/dx_3 \sim x_3^{-1}$. The data shown in Fig. 8 clearly favour the more singular behaviour predicted for the vector gluon.

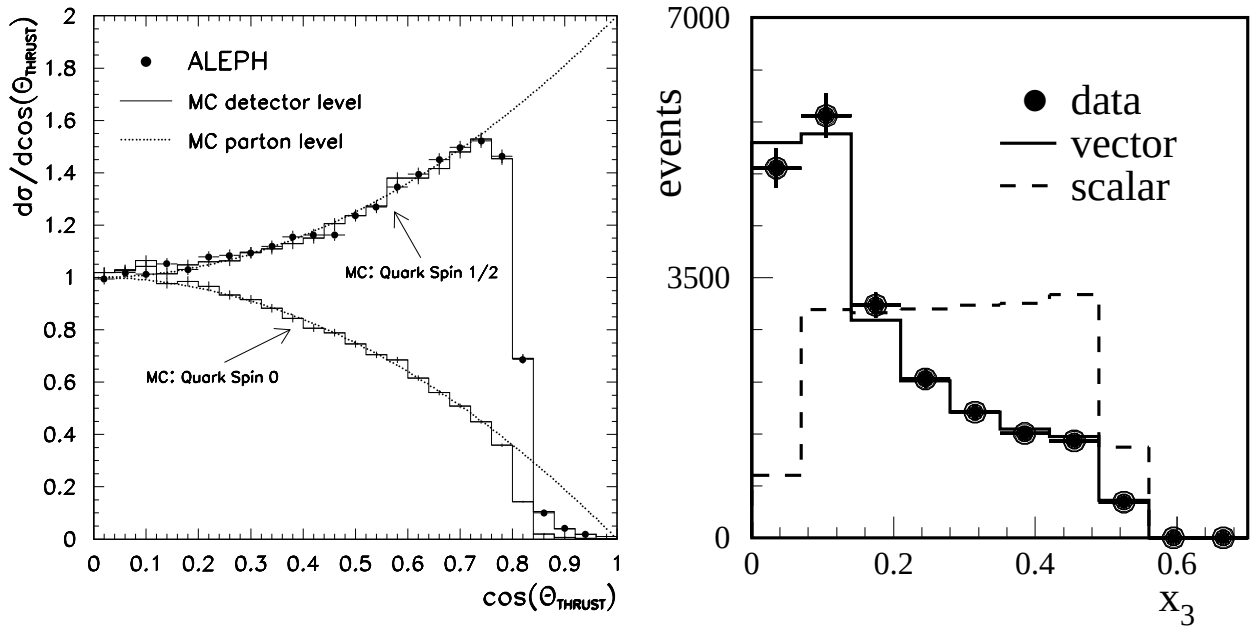

Figure 8: Distributions sensitive to the spin of the partons. The left hand plot shows the angular distribution of the thrust axis, which allows to probe the quark spin. The drop in the data above $\cos\Theta \approx 0.8$ is due to the event selection procedure. The right hand side displays the scaled–energy spectrum of the lowest energy jet in 3–jet events as measured by the L3-collaboration [77]. The experimental data are compared to predictions from a vector and a scalar gluon model.

3.2 Flavour Independence of the Strong Coupling Constant

A characteristic feature of any non–abelian gauge theory is the fact, that all interacting fermions must have the same colour charge in order to garantie gauge invariance. This is seen most easily by looking at the leading order diagrams for Compton scattering. In QED, or any other abelian theory, only the s– and u–channel exchanges with a fermion propagator contribute, which are gauge invariant for arbitrary fermion charges. In non–abelian theories in addition a t–channel exchange involving a triple gauge boson coupling contributes. Gauge invariance now requires the fermion charge to be in a fixed relation, as defined by the gauge group, to the charge carried by the gauge bosons. As a consequence, all fermions which couple to the same gauge bosons must have the same colour charge, meaning that the strong couling constant must be flavour independent.

Experimentally the flavour independence of α_s can be probed by doing a measurement of the strong coupling constant on data sets with different compositions of the primary quark flavours that couple to the Z. Requiring for instance a lepton with large p_T relative to the thrust axis, a displaced secondary vertex or large impact parameters in an event yields a b-quark enriched sample. Anti–tagging on lifetime or simply requiring a leading particle in the event with a momentum of more than 70% of the beam momentum enriches light flavours uds. Selecting a D^* or leading K^0 produces a sample enriched in c- or s-quarks, respectively. The actual flavour composition due to a specific tag is usually estimated by Monte Carlo simulations. The analysis has to take into account mass effects, which induce a slight flavour dependence of the cross sections due to phase space effects that must not be confused with a flavour dependence of the coupling strength. Tree level calculations for finite quark masses exist up to $\mathcal{O}(\alpha_s^2)$ [78].

Measurement	Result
$\alpha_s(b)/\alpha_s(udsc)$ [79]	1.002 ± 0.023
$\alpha_s(b)/\alpha_s(udsc)$ [80]	1.00 ± 0.05
$\alpha_s(b)/\alpha_s(udsc)$ [81]	1.00 ± 0.08
$\alpha_s(b)/\alpha_s(udsc)$ [82]	$0.992 \pm^{0.015}_{0.017}$
$\alpha_s(b)/\alpha_s(udsc)$ [83]	1.002 ± 0.023
Average $\alpha_s(b)/\alpha_s(udsc)$	0.997 ± 0.024
$\alpha_s(uds)/\alpha_s(bc)$ [79]	0.971 ± 0.023
$\alpha_s(uds)/\alpha_s(bc)$ [84]	1.308 ± 0.221
$\alpha_s(uds)/\alpha_s(bc)$ [83]	0.967 ± 0.101
Average $\alpha_s(uds)/\alpha_s(bc)$	0.972 ± 0.029
$\alpha_s(c)/\alpha_s^{incl}$ [84]	0.912 ± 0.091
$\alpha_s(c)/\alpha_s^{incl}$ [83]	1.012 ± 0.174
Average $\alpha_s(c)/\alpha_s^{incl}$	0.934 ± 0.103

Table 3: Tests of the flavour independence of the strong coupling constant.

Results are usually expressed as ratios of the strong coupling constant for a tagged compared to the complementary quark flavours or to the inclusive measurement for the natural flavour mix on the Z resonance. In these ratios most of the otherwise dominant theoretical errors cancel. Results are collected in Tab. 3 for $\alpha_s(b)/\alpha_s(udsc)$, $\alpha_s(uds)/\alpha_s(bc)$ and $\alpha_s(c)/\alpha_s^{incl}$. Within errors the findings are consistent with flavour universality of α_s. The most precise result is for $\alpha_s(b)/\alpha_s(udsc)$ with a relative error of 2.5%.

3.3 Colour Factors of QCD

Measurements of the colour factors of QCD allow to verify that the dynamics is described by an unbroken SU(3) gauge symmetry. The static quark model describes hadrons as bound states of quarks with three colour degrees of freedom. Assuming that these colours exhibit an SU(3) symmetry the model is able to explain the observed hadrons as colour singlet systems. Note that up to this point the concept of colour is purely static. Although it is a natural step to assume that those colours also govern the dynamics of strong interactions, i.e. building QCD on the gauge group SU(3), this is something that needs to be tested. It is for examples conceivable that not all colour degrees of freedom of the quarks contribute to the dynamics of QCD. In this case SU(2), SO(2) or U(1) become possible candidates for the gauge symmetry. Going one step further one can also imagine strong interactions to be described by a spontaneously broken SU(3) symmetry. The resulting massive gauge bosons would result in a dynamical structure which deviates from the SU(3) expectation. Deviations can also be caused by the existence of new physics, which couples to the strong interactions sector. A popular example for the latter is the case of a light gluino, the supersymmetric partner of the gluon, which at $\mathcal{O}(\alpha_s^2)$ contributes three additional fermionic degrees of freedom in e^+e^-–annihilation processes [70].

Experimentally the full gauge structure of QCD becomes accessible in $\mathcal{O}(\alpha_s^2)$. The types of diagrams contributing to the process $e^+e^- \rightarrow$ Hadrons at that order are shown on left in Fig. 9. In addition to the abelian double–bremsstrahlung diagrams (a,b) and the splitting of an intermediate gluon into a secondary quark-antiquark pair (d) there is also the process of a gluon splitting into secondary gluons (c), the defining characteristic of a non–abelian gauge theory.

The contribution of individual diagrams to the observable cross section is not gauge invariant. It is therefore not possible to experimentally isolate e.g. the triple–gluon contribution to the 4–jet cross section. A gauge invariant way to probe the structure of the underlying theory is to measure colour factors C_F, C_A and T_F. For a given representation of a gauge group describing the interaction, the colour factors are defined through the structure constants f^{abc} and the generators T^a_{ij}:

$$\sum_{a=1}^{N_A} \left(T^a T^{\dagger a}\right)_{ij} = \delta_{ij} C_F \quad , \quad \sum_{a,b=1}^{N_A} f^{abc} f^{*abd} = \delta^{cd} C_A \quad , \quad \sum_{i,j=1}^{N_F} T^a_{ij} T^{\dagger b}_{ji} = \delta^{ab} T_F. \qquad (12)$$

The colour factor C_F is the Casimir operator of the fermionic representation with dimension N_F, C_A the one of the adjoint representation of the gluons with dimension N_A. Summing over all indices in the defining equations for C_F and T_F one finds $N_F C_F = N_A T_F$, i.e. a connection between the dimensionalities of the fermionic and the gluonic representation.

In an intuitive way the colour factors can be identified with the fundamental couplings of the theory as illustrated in Fig. 9. The factor C_F determines the coupling strength of a gluon to a quark or antiquark, C_A the strength of the gluon self-coupling and T_F the probability for the splitting of a gluon into a quark-antiquark pair. In other words, C_F and C_A can be viewed as the square of the colour charge of a quark and a gluon, respectively. Absorbing a factor C_F into the definition of the coupling constant one sees, that the gauge structure of the underlying theory can be parametrized by two ratios: C_A/C_F, the ratio of gluon–self coupling to the quark–gluon coupling, and $T_F/C_F = N_F/N_A$, the number of colours caried by the quarks divided by the number of gluons.

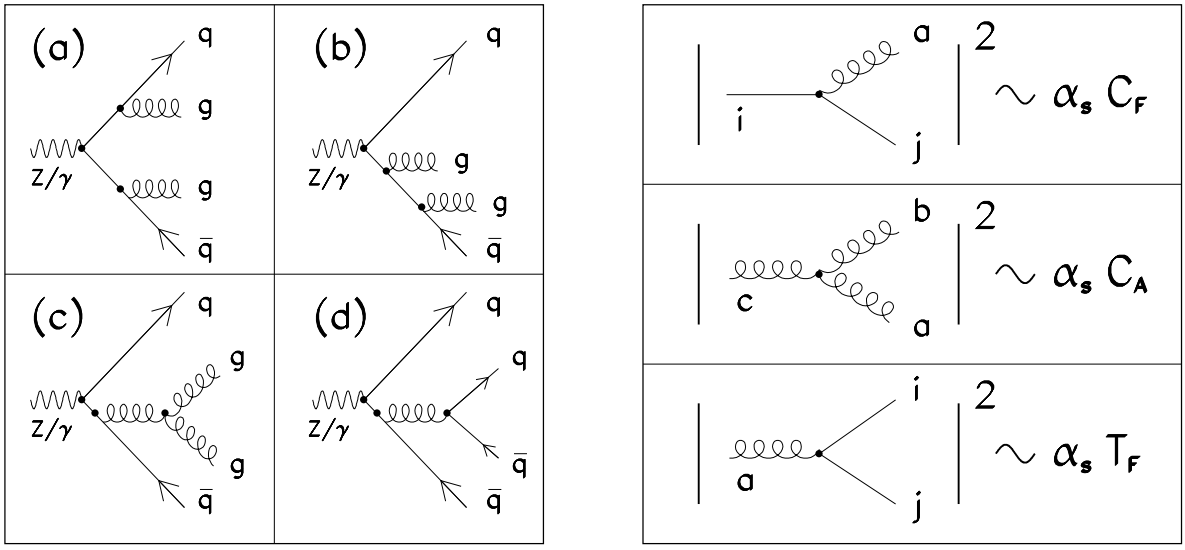

Figure 9: Generic leading order Feynman diagrams contributing to the 4–jet cross section in e^+e^--annihilation into hadrons (left hand side) and pictorial representation of the definition of the colour factors (right hand plot).

With the definitions Eq.(12) the generic form of the cross section can be written as

$$\sigma = (\alpha_s C_F) A + (\alpha_s C_F)^2 B \left(\frac{C_A}{C_F}, \frac{T_F}{C_F} n_f\right) + \mathcal{O}(\alpha_s^3), \qquad (13)$$

The function A is independent of the gauge structure. The dependence on the gauge group enters through B, which is a function of the colour factor ratios. The contributions from the

gluon–splitting process proportional to T_F/C_F is always multiplied with the number of active fermion flavours n_f. Measurements of colour factors exist based on 2–, 3– and 4–jet events. In the case of 4–jet events the coefficient A is zero and the gauge structure determines the theoretical prediction at leading order. For 2– and 3–jet events it appears in the next-to-leading order corrections, which, despite higher statistics, renders a measurement more difficult.

Two approaches are used in the analysis. The first one is an unbinned maximum likelihood fit of the colour factor ratios to the observed differential cross section [85, 86, 87]. This guaranties that all available information is used in the measurement at the expense that the quality of the fit is difficult to asses. A more intuitive approach is based on using test variables with particular sensitivity to the gauge structure of the theory. Candidate variables are discussed in [88]. Early comparisons with experimental data can be found in [89], showing that the results compatible with the QCD prediction, while an abelian toy-model, based on an $U(1)_3$ gauge symmetry could be excluded. Actual measurements of the colour factors based on test variables were done in [90, 91, 92].

Measurement	C_A/C_F	T_F/C_F	Correlation
4-Jet [85]	2.24 ± 0.40	0.58 ± 0.29	$+0.043$
4-Jet [91]	2.32 ± 0.25	0.266 ± 0.148	-0.242
4-Jet [86]	1.89 ± 0.38	0.274 ± 0.171	$+0.06$
4-Jet [92]	2.11 ± 0.32	0.40 ± 0.17	-0.450
Average (4-Jet)	2.20 ± 0.26	0.32 ± 0.14	-0.220
2&3–Jet [87]	4.49 ± 1.35	2.01 ± 0.99	$+0.945$
Average (Jet-Studies)	2.22 ± 0.22	0.33 ± 0.12	$+0.007$

Table 4: Measurements of the QCD colour factors based on jet studies in e^+e^--annihilation processes into hadrons.

The results from jet studies are collected in Tab. 4. The 4–jet results are averaged taking correlations into account using the effective procedure proposed in [73]. The 4–jet average and the 3–jet result are considered to be uncorrelated for the final average. The results are in good agreement with the QCD expectation, $C_A/C_F = 2.25$ and $T_F/C_F = 0.375$. Assuming three colours for the quarks the latter ratio corresponds to a measurement of the number of gluons $N_A = 8.8 \pm 3.3$. The combined result is displayed in Fig. 10 together with the expectation for all simple Lie–groups with the fermions in the fundamental and the gluons in the adjoint representation. Also shown is the expectation for the case of a light gluino contributing to the dynamics of QCD, which cannot yet be ruled out by jet studies alone.

Other measurements of colour factors come from $p\bar{p}$ collider data [93] or the analysis of the running of the strong couping constant [70]. That the energy evolution of α_s contains information about the underlying gauge structure is evident from Eq.(2). To fully exploit the available information in a consistent way, however, is complicated by the fact that almost all available measurements of the strong coupling constant are based on the assumption of an SU(3) gauge symmetry. A consistent analysis of the running thus would require a prior re–evaluation of the coupling constant as function of the colour factors, which in most cases is not feasible. An exception is the case of R_Z and R_τ, which are conceptually sufficiently simple to facilitate a consistent re–analysis, while at the same time being very sensitive to the running of α_s because

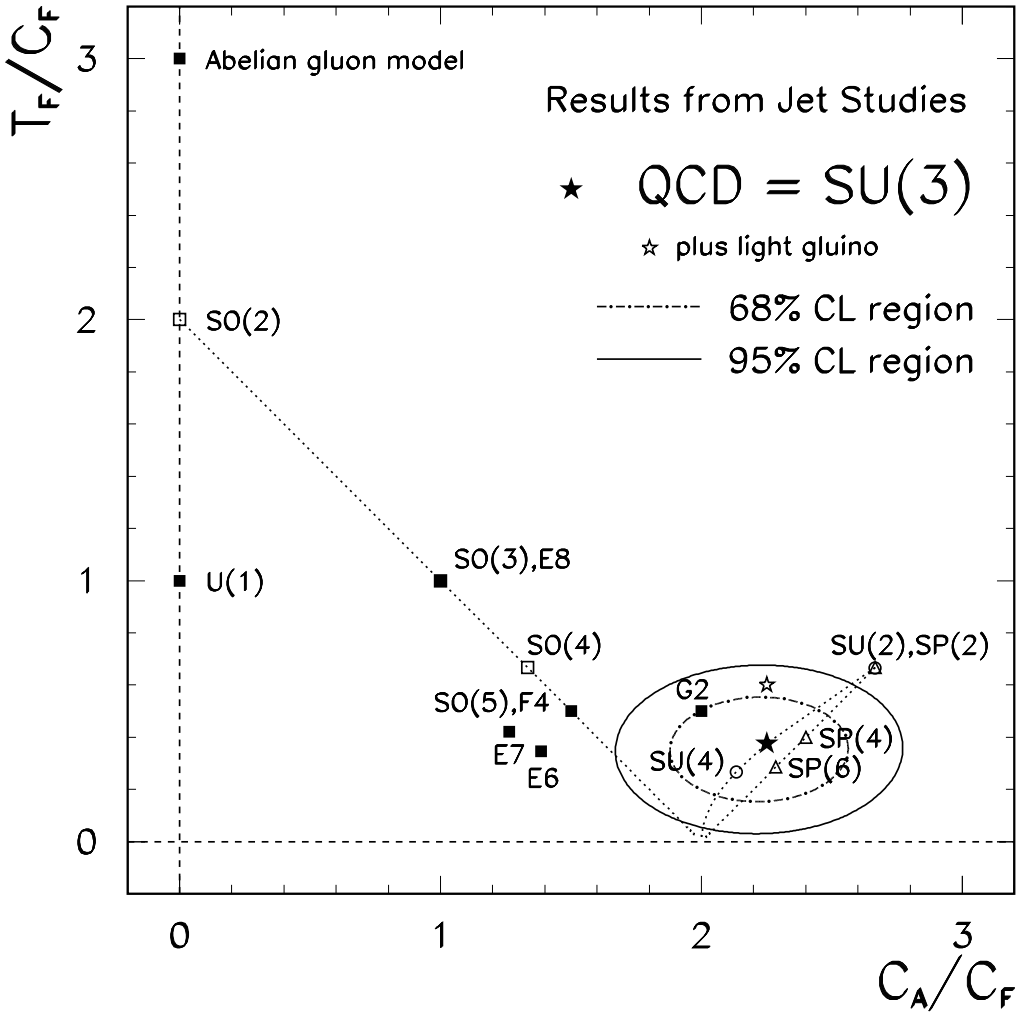

Figure 10: Combined results from colour factor measurements done at LEP based on jet-studies. In addition to the experimental 68% and 95% confidence level contours the expectations for all simple Lie groups with the fermions in the fundamental and the gluons in the adjoint representation are shown.

of the large energy range spanned. Other candidates for low-energy points could be the α_s–determinations based on sum rules. The potential of those kinds of analyses may be illustrated by doing an analysis along the lines presented in [70], using the values $R_Z = 20.800 \pm 0.035$ and $R_\tau = 3.641 \pm 0.017$ as input. Combined with the results from jet studies the errors of the colour factor measurements are reduced by almost 30%. The total size of the error ellipse is reduced even further because the colour factor ratios extracted from the analysis of the running of α_s are 100% correlated.

4 Summary

Perturbative QCD has successfully been tested in a large variety of reactions and over a large energy range, involving both space–like and time–like momentum transfers. The strong coupling constant has been found to evolve with energy as predicted by QCD, with a value consistent with the current PDG average $\alpha_s(M_Z) = 0.117 \pm 0.005$. A new average based on the measurements presented here suggest a slightly smaller error $\alpha_s(M_Z) = 0.117 \pm 0.004$. The structure of

QCD is consistent with the expectation from a gauge theory based on an unbroken SU(3) symmetry. Quarks and gluons are shown to be spin 1/2 and spin 1 particles, respectively. Within an error of 2.5% the strong coupling is found to be flavour independent. From the study of multi–jet events in e^+e^-–annihilation processes the colour factor ratios are measured as $C_A/C_F = 2.221 \pm 0.225$ and $T_F/C_F = 0.353 \pm 0.132$, compatible with the SU(3) prediction $C_A/C_F = 2.25$ and $T_F/C_F = 0.373$. Assuming three colours for the quarks, the number of gluons is measured as $N_A = 8.8 \pm 3.3$.

Acknowledegements

It is a pleasure to thank all colleagues who contributed results or inspiration for this review. In particular I would like to mention Lothar Bauerdick, Ulrich Görlach, Jutta Hartmann, Rob Kutschke, Günther Quast, Andreas Seitz, Martin Wunsch and the organizers of *Physics in Collision 1995*. Although I hope that the above review is a reasonably complete compilation of the most relevant results concerning tests of perturbative QCD, it is certainly not complete and my sincere apologies go to everybody whose work I may have missed in collecting the material.

References

[1] J.D. Bjorken and E.A. Paschos, *Phys. Rev.* 185 (1969) 1975.

[2] M.Y. Han and Y. Nambu, Phys. Rev. B139 (1965) 1006.

[3] E. Reya, *Phys. Rep.* 69 (1981) 195.

[4] H. Fritzsch, M. Gell-Mann and H. Leutwyler, *Phys. Lett.* B47 (1973) 365.

[5] ALEPH collaboration, D. Buskulic *et al.*, *Phys. Lett.* B303 (1993) 198.

[6] D.J. Gross and F. Wilczek, *Phys. Rev. Lett.* 30 (1973) 1343;
H.D. Politzer, *Phys. Rev. Lett.* 30 (1973) 1346.

[7] J. Ellis and M. Karliner, *Phys. Lett.* B341 (1995) 397.

[8] NuTeV Collaboration, D. Harris, *XXXth Rencontres de Moriond*, 19-26 March 1995.

[9] The LEP Electroweak Working Group, LEPEWWG/95-01.

[10] T. Hebbeker, M. Martinez, G. Passarino, G. Quast, *Phys. Lett.* B331 (1994) 165.

[11] CDF Collaboration, F. Abe *et al.*, FERMILAB-PUB-95/022-E;
D0 Collaboration, S. Abachi *et al.*, FERMILAB-PUB-95/028-E.

[12] G. d'Agostini, W. de Boer and G. Grindhammer, *Phys. Lett.* B229 (1989) 160.

[13] R. Marshall, *Z. Phys.* C43 (1989) 595.

[14] OPAL Collaboration, R. Akers *et al.*, CERN-PPE/95-06.

[15] M. Wunsch, private communication.

[16] ALEPH Collaboration, P. Reeves, *XXXth Rencontres de Moriond*, 19-26 March 1995;
ALEPH Collaboration, D. Buskulic *et al.*, *Phys. Lett.* B307 (1993) 209.

[17] CLEO Collaboration, D.J. Dumas, *XXXth Rencontres de Moriond*, 19-26 March 1995.

[18] M. Kobel, *XXVIIth Rencontres de Moriond*, 22-28 March 1992.

[19] P. Mackenzie, *XXXth Rencontres de Moriond*, 19-26 March 1995;
A.X. El-Khadra *et al.*, *Phys. Rev. Lett.* 69 (1992) 729,
A.X. El-Khadra, *Lattice '93*, Dallas, October 12-16, 1993;
P. Lepage and J. Sloan, *Lattice '93*, Dallas, October 12-16, 1993;
C.T.H Davies *et al.*, ICHEP94, Glasgow, 20-27 July 1994;
J. Shigemitsu, ICHEP94, Glasgow, 20-27 July 1994.

[20] DELPHI Collaboration, P. Abreu *et al.*, *Phys. Lett.* B311 (1993) 408.

[21] ALEPH Collaboration, ICHEP94, Glasgow, 20-27 July 1994, Ref.0525.

[22] H1 Collaboration, T. Ahmed *et al.*, DESY 94-220.

[23] ZEUS Collaboration, J. Hartmann and L.A.T. Bauerdick, private communication.

[24] UA2 Collaboration, J. Alitti *et al.*, *Phys. Lett.* B263 (1991) 563.

[25] D0 Collaboration, S. Abachi *et al.*, FERMILAB-PUB-95/085-E

[26] UA6 Collaboration, G. Ballocchi *et al.*, CERN-PPE/93-129.

[27] A.Geiser (UA1 Collaboration), PITHA 92/19 (1992).

[28] CLEO Collaboration, L.Gibbons *et al.*, CLNS 95-1323, CLEO 95-2.

[29] TPC/2γ Collaboration, D.A. Bauer *et al.*, ICHEP94, Glasgow, 20-27 July 1994, Ref.0254.

[30] MARK II Collaboration, S. Komamiya *et al.*, *Phys. Rev. Lett.* 64 (1990) 987.

[31] S. Bethke, LBL-28112, November 1989;
B. Naroska, *Phys. Rep.* 148 (1987) 67;
S.L. Wu, *Lepton-Photon Symposium*, Hamburg, July 27-31, 1987.

[32] TOPAZ Collaboration, I. Adachi *et al.*, *Phys. Lett.* B227 (1989) 495.

[33] AMY Collaboration, K.B. Lee *et al.*, *Phys. Lett.* B313 (1993) 469.

[34] TOPAZ Collaboration, Y. Ohnishi *et al.*, *Phys. Lett.* B313 (1993) 475.

[35] TOPAZ Collaboration, M. Aoki *et al.*, ICHEP94, Glasgow, 20-27 July 1994, Ref.0168.

[36] VENUS Collaboration, K. Abe *et al.*, *Phys. Lett.* B240 (1990) 232.

[37] SLD Collaboration, K. Abe *et al.*, *Phys. Rev.* D51 (1995) 962.

[38] ALEPH Collaboration, D. Decamp *et al.*, *Phys. Lett.* B284 (1992) 408.

[39] DELPHI Collaboration, P. Abreu *et al.*, *Z. Phys.* C59 (1993) 21.

[40] L3 Collaboration, J. Casaus, *XXXth Rencontres de Moriond*, 19-26 March 1995.

[41] OAPL Collaboration, P.D. Acton *et al.*, *Z. Phys.* C59 (1993) 1.

[42] S.G. Gorishny, A.L. Kataev and S.A. Larin, *Phys. Lett.* B212 (1988) 238.

[43] S.G. Gorishny, A.L. Kataev and S.A. Larin, *Phys. Lett.* B259 (1991) 144;
L.R. Surguladze and M.A. Samuel, *Phys. Rev. Lett.* 66 (1991) 560.

[44] W. de Boer, R. Ehret and S. Schael, preprint PITHA 94/33.

[45] E. Braaten, S. Narison and A. Pich, *Nucl. Phys.* B373 (1992) 581.

[46] F. Le Diberder and A. Pich, *Phys. Lett.* B286 (1992)147;
F. Le Diberder and A. Pich, *Phys. Lett.* B289 (1992)165.

[47] M.A. Shifman, A.L. Vainshtein, V.I. Zakharov, *Nucl. Phys.* B147 (1979) 385, 448, 519.

[48] T.N. Truong, EP-CPth.A266.1093 and preprint PITHA 94/33;
G. Altarelli, 3rd Workshop on Tau Lepton Physics, Montreux, 19-22 September 1994.

[49] W. Bernreuther and W. Wetzel, *Nucl. Phys.* B197 (1982) 228;
W. Bernreuther, *Annals of Physics* 151 (1983) 127;
W.J. Marciano, *Phys. Rev.* D29 (1984) 580;
G. Rodrigo and A. Santamaria, CERN-TH.6899/93.

[50] BCDMS Collaboration, A.C. Benvenuti *et al.*, *Phys. Lett.* B195 (1987) 97.

[51] EMC-Collaboration, S. Wimpenny *et al.*, preprint UCR DIS 91-03.

[52] NMC Collaboration, M. Arneodo *et al.*, *Phys. Lett.* B309 (1993) 222.

[53] M. Virchaux and A. Milsztajn, *Phys. Lett.* B274 (1992) 221.

[54] CHARM Collaboration, F. Bergsma *et al.*, *Phys. Lett.* B153 (1985) 111.

[55] CDHSW Collaboration, P. Berge *et al.*, *Z. Phys.* C49 (1990) 187.

[56] CCFR Collaboration, W.H. Smith *et al.*, WISC EX 93-331.

[57] M. Virchaux, *QCD 20 years later*, Aachen, 9-13 June 1992.

[58] V.N. Gribov and L.N. Lipatov, *Sov. J. Nucl. Phys.* 15 (1972) 78;
G. Altarelli, G. Parisi, *Nucl. Phys.* B126 (1977) 298;
Yu.L. Dokshitzer, *Sov. Phys. JETP* 46 (1977) 641.

[59] G. Gurci, W. Furmanski and R. Petronzio, *Nucl. Phys.* B175 (1980) 27;
W. Furmanski and R. Petronzio, CERN-TH.2933 and *Nucl. Phys.* B175 (1980) 27;
G. Altarelli, R.K. Ellis, G. Martinelli and So-Young Pi, *Nucl. Phys.* B160 (1979) 301.

[60] P. Nason and B.R. Webber, *Nucl. Phys.* B421 (1994) 473.

[61] ALEPH Collaboration, D. Busculic *et al.*, CERN-PPE / 95-096.

[62] E. Fahri, *Phys. Rev. Lett.* 39 (1977) 1587.

[63] T. Chandrahoman and L. Clavelli, *Nucl. Phys.* B184 (1981) 365.

[64] Y.L. Dokshitzer, Workshop on Jets at LEP and HERA, Durham (1990).

[65] S. Bethke, Z. Kunszt, D.E. Soper and W.J. Stirling, *Nucl. Phys.* B370 (1992) 310.

[66] F. Bloch and A. Nordsieck, *Phys. Rev.* 52 (1937) 54;
T. Kinoshita, *J. Math. Phys.* 3 (1962) 650;
T.D. Lee and M. Nauenberg, *Phys. Rev.* 133 (1964) 1549.

[67] P. Nason, Program EVENT - MC integration of ERT matrix elements.

[68] R.K. Ellis, D.A. Ross and A.E. Terrano, *Nucl. Phys.* B178 (1981) 421.

[69] S. Catani, L. Trentadue, G. Turnock and B.R. Webber, CERN-TH.6640/92.

[70] M. Schmelling and R.D. St.Denis, *Phys. Lett.* B329 (1994) 393 and CERN-PPE/93-193 .

[71] B. Bambha *et al.*, "QCD Generators for LEP", CERN-TH.5466/89.

[72] M. Schmelling, *Physica Scripta* 51 (1995) 683.

[73] M. Schmelling, *Physica Scripta* 51 (1995) 676.

[74] The Particle Data Group, *Phys. Rev.* D50 (1994) 1302.

[75] R.F. Schwitters *et al.*, *Phys. Rev. Lett.* 35 (1975) 1320;
G. Hanson *et al.*, *Phys. Rev. Lett.* 35 (1975) 1609.

[76] E. Laermann, K.H. Streng and P.M. Zerwas, *Z. Phys.* C3 (1980) 289;
E. Laermann, K.H. Streng and P.M. Zerwas, Erratum *Z. Phys.* C52 (1991) 352;
J. Ellis and I. Karliner, *Nucl. Phys.* B148 (1979) 141;
J.G. Körner, G.A. Schuler and F. Barreiro, *Phys. Lett.* B188 (1987) 272.

[77] TASSO Collaboration, R. Brandelik *et al.*, *Phys. Lett.* B97 (1980) 453;
PLUTO Collaboration, C. Berger *et al.*, *Phys. Lett.* B97 (1980) 459;
CELLO Collaboration, H.-J. Behrend *et al.*, *Phys. Lett.* B110 (1982) 329;
ALEPH Collaboration, ICHEP94, Glasgow, 20-27 July 1994, Ref.0529;
DELPHI Collaboration, P. Abreu *et al.*, *Phys. Lett.* B274 (1992) 498;
L3 Collaboration, B. Adeva *et al.*, *Phys. Lett.* B264 (1991) 551;
OPAL Collaboration, G. Alexander *et al.*, *Z. Phys.* C52 (1991) 543.

[78] B.L. Ioffe, *Phys. Lett.* B78 (1978) 277;
E. Laermann and P.M. Zerwas, *Phys. Lett.* B89 (1980) 225;
A. Ballestrero, E. Maina and S. Moretti, *Phys. Lett.* B294 (1992) 425;
A. Ballestrero, E. Maina and S. Moretti, *Nucl. Phys.* B415 (1994) 265.

[79] ALEPH Collaboration, D. Busculic *et al.*, CERN-PPE / 95-018.

[80] DELPHI Collaboration, P. Abreu *et al.*, CERN-PPE/93-59.

[81] L3 Collaboration, B. Adeva *et al.*, *Phys. Lett.* B271 (1991) 461.

[82] OPAL Collaboration, R. Akers *et al.*, CERN-PPE/94-123.

[83] SLD Collaboration, K. Abe *et al.*, SLAC-PUB-6687.

[84] OPAL Collaboration, R. Akers *et al.*, *Z. Phys.* C60 (1993) 397.

[85] ALEPH Collaboration, D. Decamp *et al.*, *Phys. Lett.* B284 (1992) 151.

[86] L3 Collaboration, L3 Note # 1726.

[87] ALEPH-Collaboration, ICHEP94, Glasgow, 20-27 July 1994, Ref.0546.

[88] J.G. Körner, G. Schierholz and J. Willrodt, *Nucl. Phys.* B185 (1981) 365;
O. Nachtmann and A. Reiter, *Z. Phys.* C16 (1982) 45;
G. Rudolph, "Physics at LEP", CERN 86-02 (1986) Vol.2, 150;
M. Bengtson and P.M. Zerwas, *Phys. Lett.* B208 (1988) 306;
M. Bengtson, *Z. Phys.* C42 (1989) 75.

[89] AMY Collaboration, I.H. Park *et al.*, *Phys. Rev. Lett.* 62 (1989) 1713;
VENUS Collaboration, K. Abe *et al.*, *Phys. Rev. Lett.* 66 (1991) 280;
ABCDHW Collaboration, A. Breakstone *et al.*, *Phys. Lett.* B248 (1990) 220;
L3 Collaboration, B. Adeva *et al.*, *Phys. Lett.* B248 (1990) 227;
OPAL Collaboration, M.Z. Akrawy *et al.*, *Z. Phys.* C49 (1991) 49.

[90] DELPHI Collaboration, P. Abreu *et al.*, *Phys. Lett.* B255 (1991) 466;
DELPHI Collaboration, P. Abreu *et al.*, *Z. Phys.* C59 (1993) 357.

[91] DELPHI Collaboration, ICHEP94, Glasgow, 20-27 July 1994, Ref.0180;
A. Seitz, private communication.

[92] OPAL Collaboration, CERN-PPE/94-195.

[93] Achim Geiser, CERN-PPE/94-38.